Current Research in Food Science 6 (2023) 100463

Contents lists available at ScienceDirect

Current Research in Food Science

journal homepage: www.sciencedirect.com/journal/current-research-in-food-science

Curcumin encapsulated zein/caseinate-alginate nanoparticles: Release and antioxidant activity under *in vitro* simulated gastrointestinal digestion

Yunfei Huang [a], Yiling Zhan [a], Guangyi Luo [a], Yan Zeng [a], David Julian McClements [b,*], Kun Hu [a,**]

[a] Food Science School, Guangdong Pharmaceutical University, Zhongshan, 528458, China
[b] Department of Food Science, University of Massachusetts, Amherst, MA, 01003, USA

ARTICLE INFO

Handling Editor: Professor A.G. Marangoni

Keywords:
Curcumin
Zein nanoparticles
pH-shifting
Bioaccessibility
Antioxidant activity

ABSTRACT

Curcumin-loaded zein/sodium caseinate-alginate nanoparticles were successfully fabricated using a pH-shift method/electrostatic deposition method. These nanoparticles produced were spheroids with a mean diameter of 177 nm and a zeta-potential of −39.9 mV at pH 7.3. The curcumin was an amorphous, and the content in the nanoparticles was around 4.9% (w/w) and the encapsulation efficiency was around 83.1%. Aqueous dispersions of the curcumin-loaded nanoparticles were resistant to aggregation when subjected to pH changes (pH 7.3 to 2.0) and sodium chloride addition (1.6 M), which was mainly attributed to the strong steric and electrostatic repulsion provided by the outer alginate layer. An *in vitro* simulated digestion study showed that the curcumin was mainly released during the small intestine phase and that its bioaccessibility was relatively high (80.3%), which was around 5.7-fold higher than that of non-encapsulated curcumin mixed with curcumin-free nanoparticles. In the cell culture assay, the curcumin reduced reactive oxygen species (ROS), increased superoxide dismutase (SOD) and catalase (CAT) activity, and reduced malondialdehyde (MDA) accumulation in hydrogen peroxide-treated HepG2 cells. The results suggested that nanoparticles prepared by pH shift/electrostatic deposition method are effective at delivering curcumin and may be utilized as nutraceutical delivery systems in food and drug industry.

1. Introduction

Cucumin is a hydrophobic polyphenol which is mainly extracted from the rhizome of *Curcuma longa*(Rauf et al., 2018). It was used as food colorant and spice, as well as for its medicinal qualities for centuries in China and India. In recent years, lots of studies has proved that curcumin has antioxidant, antimicrobial, anti-inflammatory, anticancer, liver protective, neuroprotective, cardioprotective, anti-obesity, and anti-angiogenesis activities (Ak and Gulcin, 2008; Sahebkar, 2016; Rauf et al., 2018; Peng et al., 2022). Despite its multiple bioactivities, curcumin has poor bioavailability because of its insolubility in water, poor chemical stability, and fast metabolized under physiological conditions (Anand et al., 2007). For instance, a maximum curcumin concentration of 0.06 μg/mL was observed in serum even oral administration of 500 mg/kg of curcumin to rats (Peng et al., 2022).

Delivery systems were used to increase the solubility, stability, and bioavailability of curcumin including biopolymer particles, solid lipid nanoparticles, nanogels, cyclodextrin complexes, and nanoemulsions, etc (Sun et al., 2013; Liu et al., 2020). Food protein nanoparticles, specially zein nanoparticles, were also reported to encapsulate curcumin (Pan and Zhong, 2016; Peng et al., 2020). The polypeptide chain in zein consists of more than 50% of hydrophobic amino acids, which makes it insoluble in water but soluble in high ethanol aqueous solutions (60–90%)(Shukla, 2001). These solubility properties of zein as used to encapsulate curcumin in zein nanoparticles using an antisolvent precipitation method. Simply, zein and curcumin are solubilized in an aqueous ethanol solution (solvent), and this solution is then dispersed into water (antisolvent), which makes the hydrophobic zein molecules aggregate into nanoparticles that trap the hydrophobic curcumin inside (Hu et al., 2015; Hasankhan et al., 2020). However, the high hydrophobic surface of zein nanoparticles may drive particles to aggregate in aqueous solutions by hydrophobic interaction, especially when the pH

* Corresponding author.
** Corresponding author.
E-mail addresses: mcclements@foodsci.umass.edu (D.J. McClements), huk88@126.com (K. Hu).

https://doi.org/10.1016/j.crfs.2023.100463
Received 5 January 2023; Received in revised form 4 February 2023; Accepted 14 February 2023
Available online 18 February 2023

moves towards their isoelectric points (Patel et al., 2010). Moreover, they are also difficult to disperse when the nanoparticle dispersion is dehydrated and then rehydrated. This shortage can be solved by using small molecule surfactants (Dai et al., 2017; Wang et al., 2019), proteins (Patel et al., 2010; Zhu et al., 2022), polysaccharides (Hu et al., 2015; Zhang et al., 2021; Ghobadi-Oghaz et al., 2022), or protein/polysaccharide complexes (Chang et al., 2017; Yao et al., 2018) to stabilize zein nanoparticles.

Although the antisolvent precipitation method is easy to use, it is difficult to scale up and utilizes large quantities of flammable ethanol, which also needs to be removed from the final particle dispersion. Pan and co-workers reported that zein nanoparticles could be formed using a pH-shift method (Pan and Zhong, 2016), which was an alternative method of antisolvent precipitation. It is typically implemented by mixing zein and sodium caseinate at pH 11.5 and then adjusting the solution to neutral pH value, which promotes the spontaneous self-aggregation of the zein molecules(Pan and Zhong, 2016). This self-aggregation effect is linked to the change in surface charge of the zein molecules with pH: they are strongly negatively charged under alkaline conditions but only have a weak negative charge under neutral conditions, consequently the electrostatic repulsion between them is reduced (Shukla, 2001). The sodium caseinate is included in the formulation because it adsorbs to the surfaces of the zein nanoparticles after they form and reduces the surface hydrophobicity of zein particles. Moreover, its presence at the nanoparticle surfaces increases the electrostatic repulsion and steric hindrance between them which keeps particles against aggregation.

Although curcumin is insoluble in water, it can solubilize in strongly alkaline solutions (pH > 10) because it becomes partly deprotonated and gains a negative charge, thereby increasing its hydrophilicity (Pan et al., 2014). This attribute makes it possible to use the pH-shift method to fabricate curcumin encapsulated zein nanoparticles by adjusting curcumin-zein co-solubilized alkaline solution to neutral or acidic pH. These nanoparticles can be stabilized against aggregation by including an amphiphilic surfactant or charged polymer such as rhamnolipids, tea saponin, whey protein, or propylene glycol alginate (Dai et al., 2018; Zhan et al., 2020; Yuan et al., 2021; Li et al., 2022).

Sodium caseinate (NaCas) has been shown to be a particularly good stabilizer of zein nanoparticles because it gives good stability against heat and high ionic strengths (Patel et al., 2010; Chang et al., 2017). However, zein/caseinate nanoparticles precipitate at pH values near the isoelectric point of the outer caseinate layer (*i.e.,* pH 4 to 5.5) (Zou et al., 2021). This precipitation can be prevented by coating the zein/caseinate nanoparticles with anionic polysaccharides, such as κ-carrageenan (Zou et al., 2021) or sodium alginate (Liu et al., 2019). The presence of these polysaccharides improves the stability of the nanoparticles against aggregation by forming a thick anionic coating around them which increases the electrostatic repulsion and steric hindrance between the nanoparticles (Zou et al., 2021).

The adverse effect of the pH-shift method is that additional salts (usually sodium chloride) are introduced into the system when the pH is adjusted from strongly alkaline to neutral conditions. The resulting high levels of salt might reduce the electrostatic attraction between the anionic polysaccharide and the caseinate at the nanoparticle surfaces, thereby causing the polysaccharide molecules to be fully or partially displaced. As a result, the nanoparticles may no longer be protected, or they may even aggregate through bridging effects, *i.e.,* a polysaccharide attaching to the surfaces of more than one nanoparticle(Hu and McClements, 2015). There have few reports on the stability change of nanoparticles fabricated by the pH shift method when subjected to environmental stress such as pH change and ionic strength. Moreover, there have been few studies on the behavior of curcumin-loaded nanoparticles produced using this method within the gastrointestinal tract. For instance, the retention, release, bioaccessibility, and activity of curcumin in these biopolymer nanoparticles under gastrointestinal conditions is still not well understood. For this reason, we prepared curcumin-loaded zein/NaCas-sodium alginate nanoparticles with the pH shift method, and then investigated their stability when subjected to changes in pH and ionic strength. We then characterized the release, bioaccessibility, and antioxidant activity of these curcumin-loaded nanoparticles during *in vitro* simulated gastrointestinal digestion. The study may help to develop zein-based delivery systems without the need for an organic solvent.

2. Materials and methods

2.1. Materials

Zein, sodium caseinate, sodium alginate, curcumin (>98%), and Trolox (>97%) were obtained from Acros Organics (New Jersey, USA). 1, 1-Diphenyl-2-picrylhydrazyl free radical (DPPH·, >97%) and 2, 2′-azino-bis (3- ethyl-benzothiazoline-6-sulfonic acid) diammonium salt (ABTS, >98%) were obtained from TCI (Tokyo, Japan). Bile salts, pancreatin (from porcine pancreas, 8 × USP specifications), and pepsin (from porcine gastric mucosa, 535 U/mg) were obtained from Sigma-Aldrich (St Louis, MO, USA). Ascorbic acid (99%) was obtained from InnoChem Science & Technology (Beijing, China). A radioimmunoprecipitation assay buffer (RIPA) was obtained from Solarbio (Beijing, China). Cell counting kit-8 (CCK-8) and Dulbecco's Modified Eagle Medium (DMEM) were obtained from Gibco (Shanghai, China). Fetal bovine serum (FBS), penicillin-streptomycin solution, and 0.25% trypsin-0.04% EDTA were purchased from Hyclone (South Logan, Utah, USA). 2, 7-dichlorofluoroescin diacetate (DCF-DA) was purchased from MedChemExpress, USA. Test kits of superoxide dismutase (SOD), catalase (CAT), and malondialdehyde (MDA) were purchased from Jiancheng Bioengineering Institute (Nanjing, China).

2.2. Curcumin-loaded nanoparticles preparation

Zein/NaCas nanoparticles loaded with curcumin were prepared using a method described previously with some modifications (Pan and Zhong, 2016). Zein was dispersed in alkali water (pH 12.5) with the concentration of 0.5% (w/v), and the dispersion was adjusted to pH 12.5 using NaOH solution and then magnetically stirred at 900 rpm (RO5, IKA, China) for 30 min to ensure full solubilization. Then, curcumin was added into the zein solution at a concentration of 0.1% (w/v) and stirred for another 30 min. Afterward, 10 mL of zein-curcumin solution was syringe-injected into 30 mL sodium caseinate solution (0.1%, w/v) with constant stirring at 1200 r/min for 5 min. The resulting mixture was adjusted to pH 7 using 2 M HCl solution, which led to the formation of a curcumin-loaded zein/NaCas nanoparticle dispersion. This dispersion was then mixed with an equal volume of 0.2% (w/v) sodium alginate solution at 800 r/min for 5 min. The resulting mixture (pH 7.3) was then centrifuged at 3000 g (Sorvall® RC-6 Plus, Thermo, USA) for 20 min to separate any non-encapsulated curcumin and large particles. The curcumin-loaded zein/NaCas-alginate nanoparticle dispersion was then analyzed directly or was freeze-dried (Shanghai Lichen, LC-10N-50A) and stored at −20 °C for later use.

2.3. Nanoparticle characterization

2.3.1. Particle diameter and charge measurements

The average diameter, polydispersity index (PDI), and ζ-potential of the nanoparticle dispersions were determined by a Nano-ZS 90 instrument (Malvern Panalytical, UK) as reported previously (Zou et al., 2021). The samples were moderately diluted before testing.

2.3.2. Scanning electron microscopy (SEM) analysis

The microstructures of the nanoparticles were observed using a field emission scanning electron microscope (JSM-7610F PLUS, JEOL, Japan) operating at an accelerating voltage of 15.0 kV, samples were sputter-coated with gold before testing.

2.3.3. X-ray diffraction

The physical state of curcumin in freeze-dried nanoparticles, physical mixture with same compositions of curcumin, zein, caseinate, and alginate of nanoparticles was determined by an X-ray diffraction instrument (Empyrean, Malvern Panalytical, Netherland). A Cu Kα radiation source was operated at a voltage of 45 kV and a current of 40 mA, the scanning step was 0.02° with a scanning speed of 10°/min. The 2θ scan range was 5° −80°.

2.3.4. Curcumin loading amount (LA) and efficiency (LE) determination

The curcumin loading amount and efficiency of the nanoparticles were determined using a previously described method with some modifications (Yao et al., 2018). Briefly, 5 mg of freeze-dried nanoparticles was dissolved in 10 mL of dimethyl sulfoxide (DMSO) and stirred for 4 h in the dark (700 r/min). The centrifuged (3000 g, 10 min) supernatant was moderately diluted with DMSO and the absorbance was measured at 433 nm using a UV spectrophotometer (UV-1800, Shimadzu, Japan)(Zou et al., 2021). The curcumin concentration of nanoparticle solution was calculated with a standard curve of absorbance *versus* curcumin concentration at a range of 0–16 μg/mL ($R^2 = 0.999$). The loading amount and efficiency of curcumin were calculated with equations (1) and (2):

$$\text{LA}\ (\%) = \frac{\text{Mass of curcumin in nanoparticles}}{\text{Mass of nanoparticles}} \times 100 \quad (1)$$

$$\text{LE}\ (\%) = \frac{\text{loaded curcumin}}{\text{Total curcumin used}} \times 100 \quad (2)$$

2.4. Particle stability determination

The nanoparticle dispersion stability was measured when exposure to changes in solution pH or ionic strength as previously reported with some modification(Zou et al., 2021). The pH stability of freshly prepared particle dispersions was immediately determined after their pH values were adjusted ranged from pH 2.0 to 8.0 with HCl or NaOH solutions. The effect of salt on particle stability was determined by adding sodium chloride into particle dispersions reaching salt concentrations ranged from 0 to 1.6 M NaCl. The view appearance of particle dispersion was recorded with a digital camera.

2.5. In vitro simulate gastrointestinal digestion

The curcumin releasing behavior and bioaccessibility of curcumin-loaded nanoparticles was determined with a *in vitro* simulated gastrointestinal digestion model described in previous methods (Huang et al., 2019). A physical mixture containing the same amount of non-encapsulated curcumin as nanoparticles was used for comparison.

Gastric phase: nanoparticles or physical mixture were mixed with 20 mL of double distilled water to reach a curcumin concentration of 0.5 mg/mL and warmed to 37 °C in a water bath shaker. Then, these samples were mixed with 20 mL of prewarmed simulated gastric fluids (acidified water (pH 1.2) containing 50 mM NaCl and 3.2 mg/mL pepsin)(Yao et al., 2018), and the pH value was rapidly adjusted to pH 2.0. The gastric digestion was proceeded with continuously shaken at 80 rpm in a shaking incubator at 37 °C (THZ-82, Shanghai, China), and the samples were heated to inactivate pepsin (90 °C for 5 min) after *in vitro* digestion.

Small intestinal phase: The samples (42.5 mL) which finished the whole gastric digestion phase were adjusted to pH 7.0, while maintaining them at 37 °C with constant magnetic stirring (100 r/min). Then, 4 mL of bile salt solution (15.57 mg/mL bile salt solution in 5 mM PBS, pH 7.0) and 2.5 mL of pancreatin solution (48 mg/mL pancreatin in 5 mM PBS, pH 7.0) were added(Huang et al., 2019). The pH values of samples were maintained at pH 7.0 with an automatic titration instrument (902 Titrando, Metrohm, Switzerland). The digested samples were heated to inactive the pancreatin in a water bath at 90 °C for 5 min.

Bioaccessibility: The amount of curcumin was measured after the samples were incubated for 0, 20, 40, 80, and 120 min in simulated gastric fluids and for 20, 40, 80, 120, 180, and 240 min in simulated small intestinal fluids(Huang et al., 2019). The digested fluids were centrifuged at 10,000 g, 15 °C for 15 min, and the supernatants were collected and diluted with DMOS to determine the curcumin concentration described in Section 2.3.4. The percentage of curcumin released from the nanoparticles into the digestion supernatant was calculated with equation (3) (Yao et al., 2018):

$$\text{Percentage Released} = \frac{\text{Mass of released curcumin in supernatant}}{\text{Mass of curcumin before digestion}} \times 100\ \% \quad (3)$$

2.6. In vitro antioxidant capacity of digested nanoparticles

The *in vitro* antioxidant capacity of the supernatants collected after *in vitro* digestion was measured using radical scavenging methods. The supernatants consisted of the whole of the fluids collected after the whole simulated gastrointestinal digestion process.

2.6.1. DPPH· scavenging capacity assay

The DPPH· scavenging capacity of the digestion supernatant was determined as described previously (Liang et al., 2022). Briefly, 2 mL of diluted supernatant and 2 mL of DPPH· solution (100 μM) were mixed and incubated in the dark at room temperature. After 30 min, the absorbance of the solution was measured using a UV–visible spectrophotometer at 517 nm. The DPPH· scavenging percentage of the samples was quantified with equation (4):

$$\text{DPPH}\cdot\text{Scavenging}(\%) = \frac{\text{A0} - \text{As}}{\text{A0}} \times 100\% \quad (4)$$

A_0 and A_S are the absorbances of the control and sample solutions, respectively. A standard curve of ascorbic acid concentration (0–0.5 mM) *vs* DPPH· scavenging percentage was established, and the scavenging capacity of the digestion supernatant was transferred into ascorbic acid equivalents (AAE).

2.6.2. $ABTS^{+}$· scavenging ability

The $ABTS^{+}$· scavenging activity of the digestion supernatants was measured with method described previously (Liang et al., 2021, 2022). The ABTS stock solution (7 mM) was mixed with a 2.5 mM potassium persulfate solution in equal volume and stored in the dark for 16 h at ambient temperature. The resulting $ABTS^{+}$· solution was diluted with 10 mM PBS (pH 7.4) to reach an absorbance of 0.70 (±0.02) cm^{-1} at 734 nm and 30 °C(Liang et al., 2022). Then 40 μL of diluted supernatant was dissolved in 4 mL of $ABTS^{+}$· solution and reacted for 6 min, the absorbance was determined at 734 nm(Liang et al., 2021). The radical scavenging capacity of the digestion supernatants was determined using equation (5):

$$ABTS^{+}\bullet\ \text{scavenging rate}\ (\%) = \frac{\text{Ac} - \text{As}}{\text{Ac}} \times 100\% \quad (5)$$

A_C and A_S are the absorbances of the control solution and samples, respectively. A standard curve of Trolox concentration (0–2.5 mM) *vs* $ABTS^{+}$· scavenging percentage was established, and the Trolox equivalent concentration (TEC) values of the digestion supernatants were calculated.

2.7. Intracellular antioxidant activity

2.7.1. Cytotoxicity determination

HepG2 cells were cultured in DMEM containing 10% FBS and 1% penicillin-streptomycin at a density of 1×10^4 cells per well at 37 °C supplied with a humidified atmosphere containing 5% CO_2 (Peng et al., 2022). The cell culture media were aspirated after 24 h incubating and

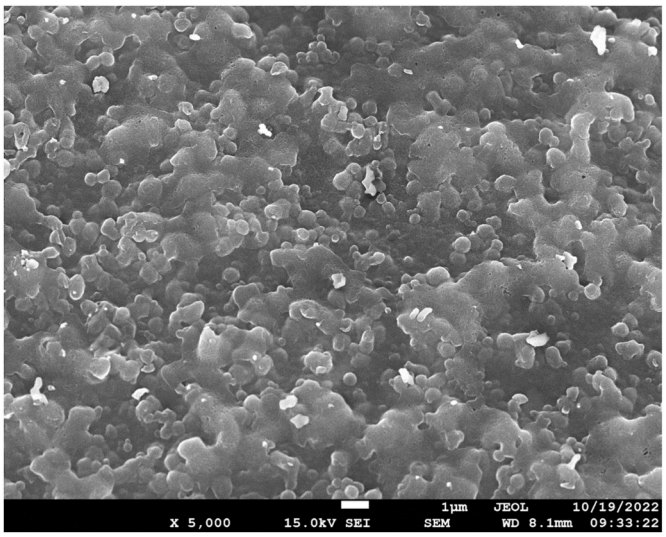

Fig. 1. SEM image of curcumin-loaded zein/caseinate-alginate nanoparticles after freeze-dried.

the cells were treated with 100 μL of culture media containing digestion supernatant (diluted with DMSO) at various concentrations for another 24 h. Cells with no digestion supernatant added were used as a control. Then, the cells were washed with PBS twice and incubated with 100 μL DMEM (containing CCK-8) for 2 h(Peng et al., 2022). The optical density (OD) values were determined at 450 nm (BioTek Instruments Inc., VT, USA).

2.7.2. Intracellular ROS determination

A H_2DCF-DA assay was used to determine the intracellular level of ROS (Huang et al., 2019). Cells were seeded in a 6 well plate with about 6×10^5 cells/well and incubated for 24 h. Then, 2 mL of digestion supernatant (from curcumin-loaded nanoparticles or curcumin physical mixtures) was diluted 50-fold with DMEM added into each well of the experimental group, and 2 mL of DMEM was added to the hydrogen peroxide (H_2O_2) model group or control group. After 2 h incubation, cell wells were treated with 2 mL of H_2O_2 (except the control group) for 30 min and washed 3 times with fresh medium. Then, each well was added with 2 mL of DCFH-DA (10 μM) and incubated for 30 min. Lastly, the cells were washed twice with PBS and imaged using fluorescence microscopy (CKX41, OLYMPUS, Japan). The fluorescent intensity was determined with a microplate reader (Synergy H1, Bio-Tek, USA) at an excitation and emission wavelength of 488 nm and 525 nm, respectively. The relative fluorescent intensity was compared to the control (Huang et al., 2019).

2.7.3. Intracellular related enzymes and MDA

Cells were seeded with about 6×10^5 cells/well and incubated for 24 h. Then, 2 mL of digestion supernatant (from curcumin-loaded nanoparticles or curcumin/nanoparticle physical mixtures) was diluted 50-fold with DMEM by adding it into each well of the experimental group, and 2 mL of DMEM was added to the H_2O_2 model group or control group. After 24 h incubation, cells were treated with 2 mL of H_2O_2 for 4 h (except the control). Lastly, the cells were lysed on ice for 30 min, centrifuged at 2500 r/min at 4 °C for 10 min to collect the supernatant. The enzymatic activities of SOD, CAT, and MDA level in the cells were measured with the instructions of the test kit supplier.

2.8. Statistical analysis

All experiments were carried out three times, and data were expressed as the mean ± standard deviation and analyzed using one-way ANOVA with Tukey's test using SPSS software (IBM SPSS statistics 19) to compare the significance among samples at a P-level of 0.05.

3. Results and discussion

3.1. Particle characteristics

Immediately after preparation, the nanoparticle dispersions had a transparent yellowish appearance and a pH of 7.3. Light scattering and zeta-potential measurements indicated that the nanoparticles had a mean size of 177.0 ± 3.8 nm, a PDI of 0.32 ± 0.04, and a ζ-potential of −39.9 ± 1.2 mV. The SEM images indicated that the nanoparticles in the freeze-dried samples were approximately spherical and had dimensions of a few hundred nanometers (Fig. 1). Many of the nanoparticles appeared to be fused together in these images, which was probably caused by the freeze-drying procedure. The curcumin content in the nanoparticles was 4.89 ± 0.01%, and the curcumin encapsulation efficiency was 83.1 ± 8.5%, which was higher than zein/caseinate-alginate nanoparticles prepared by the antisolvent precipitation method reported previously (Liu et al., 2019)

3.2. Physical state of curcumin in nanoparticles

The XRD spectrums of pure curcumin, curcumin in nanoparticles, and in physical mixture with same composition of zein, caseinate, and alginate were compared (Fig. 2A). Strong diffraction peaks were observed for pure curcumin at 2θ angles of 9.00°, 17.31°, 18.21°, and there were more peaks at the angle range of 20° to 30°, which meant that curcumin was a crystal form. The peaks at 9.00°, 17.31°, and 18.21° were also observed and weak in the spectrum of physical mixture containing curcumin, and the other peaks were too weak to be observed, which was because of the low curcumin content in the physical mixture (4.89%, w/w). The characteristic peaks of curcumin at 9.00°, 17.31°, and 18.21° were disappeared in the spectrum of nanoparticles although the curcumin content was same to the physical mixture (4.89%), which meant that curcumin was encapsulated in nanoparticle was an amorphous form. Some new peaks at 27.36°, 31.72°, 45.50°, 56.49°, and 75.37° were observed in the spectrum of nanoparticles, these peaks were the characteristic X-ray diffraction peaks of sodium chloride crystal (Fig. 2B). The sodium chloride in the nanoparticles was produced by the pH-shifting fabrication process.

3.3. Nanoparticle stability at different pH or ionic strength conditions

It is usually important that nanoparticle-based delivery systems are resistant to aggregate when subjected to environmental stress, such as pH or ionic strength changes. The curcumin-loaded zein/NaCas-alginate nanoparticles in this study were found to be stable from pH 2.0 to 7.3. The particle dispersions appeared transparent from pH 7.3 to 4.0 but became slightly turbid at pH 3.0 to 2.0 (Fig. 3A). The mean particle diameter was between 154 and 189 nm from pH 7.3 to 4.0 but increased to 336 nm at pH 2.0 ($P < 0.05$). The polydispersity index of the nanoparticles ranged from 0.19 to 0.32 ($P < 0.05$), which meant that the particle size was fairly uniform. The superior stability of these systems can mainly be attributed to the outer layer of alginate around the nanoparticles, as this provides a strong electrostatic and steric repulsion between them, which inhibits aggregation(Sani et al., 2022).

The ζ-potential of the zein/NaCas-alginate nanoparticles changed from strongly negative at neutral conditions (around −40 mV) to weakly negative at strongly acidic conditions (around −4 mV) (Fig. 3B). The fact that the nanoparticles were negatively charged throughout the whole pH range was caused by the adsorbed alginate molecules at their surfaces. The decrease in the negative charge with pH decreasing can be attributed to two phenomena: (i) the protonation of anionic carboxyl groups (-COOH) on the alginate and protein molecules; (ii) the protonation of amino groups ($-NH_3^+$) on the protein molecules (Hu et al., 2015).

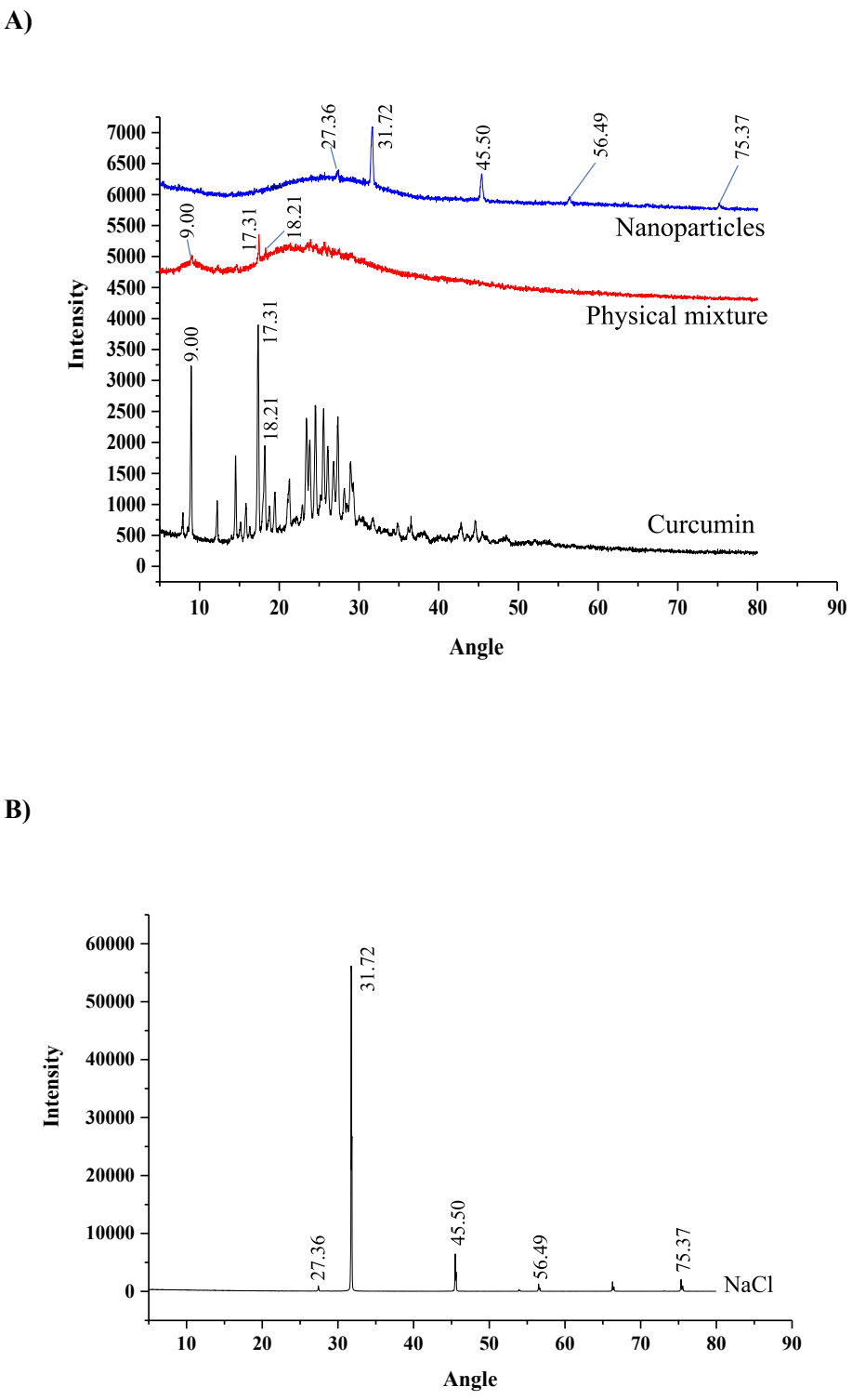

Fig. 2. XRD spectrums of: A) curcumin, nanoparticles, and physical mixture with same compositions of curcumin, caseinate, and alginate of nanoparticles; B) sodium chloride.

The magnitude of the particle surface potential is important because it influences their tendency to aggregate. At high pH values, the strong negative charge inhibits nanoparticle aggregation by generating a strong electrostatic repulsion. At low pH values, however, the much weaker negative charge may no longer be sufficient to inhibit aggregation. As a result, some of the nanoparticle aggregate, which leads to an increase in mean particle size and turbid appearance of the nanoparticle dispersions.

The effect of sodium chloride concentration on nanoparticle stability is shown in Fig. 3C. The particle dispersions were transparent at all investigated salt concentrations of 0–1.6 M NaCl, and the mean particle diameter slightly increased to 198.6 nm ($P < 0.05$) (Fig. 2C). The result is consistent with previous studies (Zou et al., 2021), where it was reported that quercetin-loaded zein/caseinate-κ-carrageenan nanoparticles prepared by the antisolvent method were stable up to sodium chloride concentrations of 2.0 M. In contrast, zein/pectin or

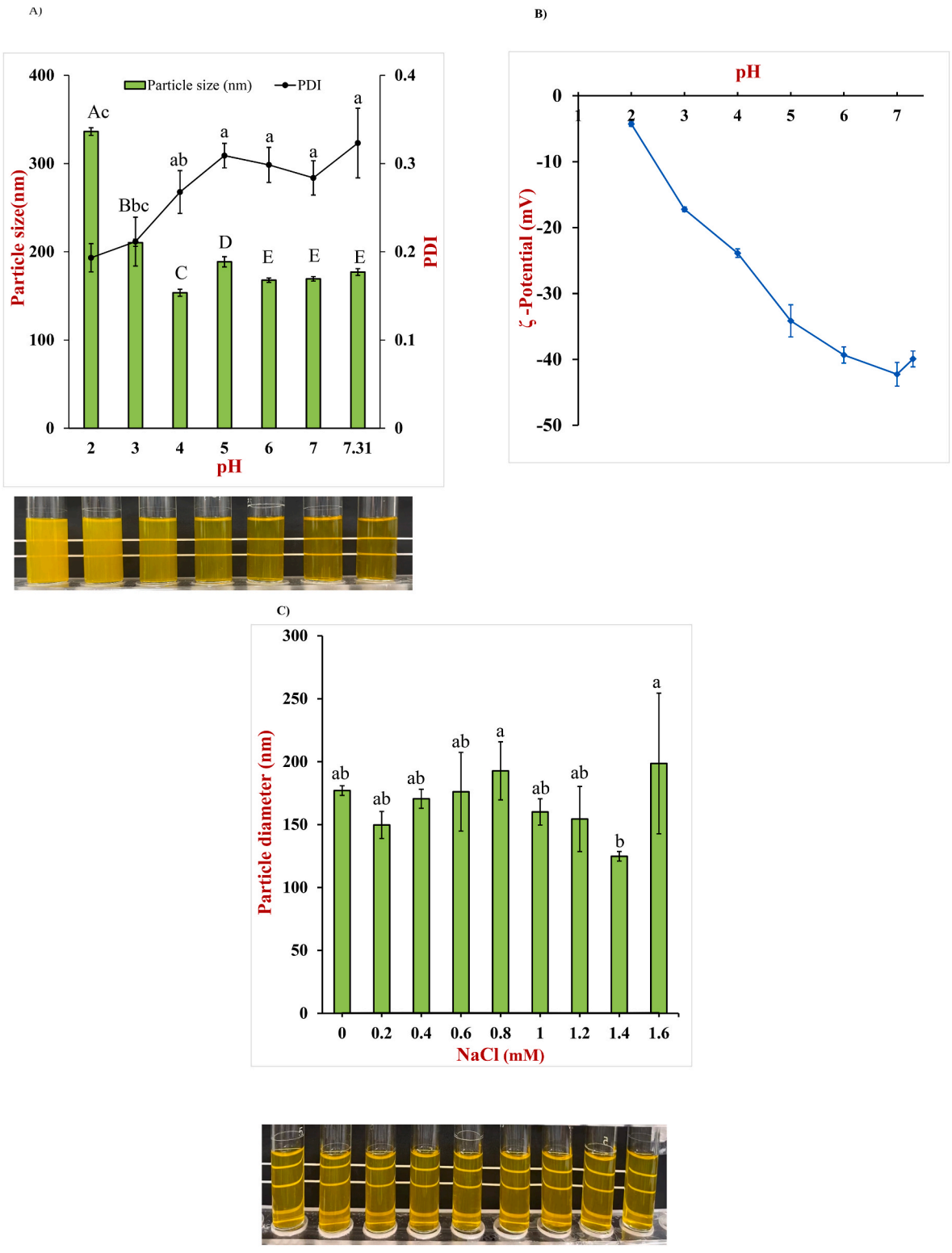

Fig. 3. Effect of pH and ion strength on the average diameter, polydispersity index, and ζ-potential of curcumin-loaded nanoparticles; A), particle diameter and PDI at different pH values ($P < 0.05$). The photograph shows the appearance of the nanoparticle dispersions from pH 2.0 to 7.31 (from left to right); B), zeta-potential of nanoparticles at pH 2.0 to 7.3; C), sodium chloride concentration on the average diameter of curcumin-loaded nanoparticles ($P < 0.05$), The photograph shows the appearance of nanoparticle dispersions containing 0–1.6 M NaCl (from left to right).

zein/alginate nanoparticles aggregated when the NaCl concentration was 100 mM or higher (Huang et al., 2016). These differences in aggregation stability suggest that sodium caseinate was critical in stabilizing nanoparticles against high ionic strengths.

3.4. Curcumin release during in vitro simulated gastrointestinal digestion

The release behavior of curcumin from nanoparticle-based delivery systems in the gastrointestinal tract is important for determining its efficacy. For this reason, curcumin release was monitored when the

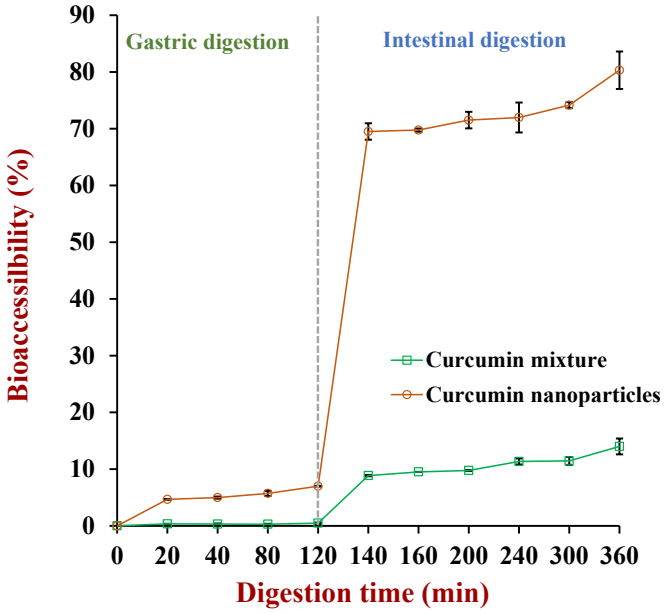

Fig. 4. Curcumin release for nanoparticles and curcumin mixture during *in vitro* stimulated gastric and intestinal digestion.

nanoparticles were exposed to simulated gastric and small intestinal conditions. In addition, the bioaccessibility of the curcumin in the final fluids resulting from simulated gastrointestinal digestion was measured. A physical mixture consisting of non-encapsulated curcumin powder and ingredients to fabricate nanoparticles was used as a comparison.

The percentage release of the curcumin from the physical mixture was relatively low 0.47 ± 0.12% after 2 h gastric digestion (Fig. 4) but it increased to 8.86 ± 0.12% after 20 min *in vitro* small intestinal digestion, and then gradually increased to 14.0 ± 1.4% after 4 h of digestion. These values are significantly higher than that of pure curcumin (Yao et al., 2018), which suggests that the digestion of the zein-based nanoparticles may have increased the solubility of the curcumin the gastrointestinal fluids. This may have been attributed to solubilization and emulsification effect of peptides produced by protein digestion (Yao et al., 2018). Even so, the final bioaccessibility of the non-encapsulated curcumin was still relatively low compared to the encapsulated curcumin.

The percentage release of the curcumin from the nanoparticle-based delivery systems was 4.67 ± 0.08% after 20 min *in vitro* gastric digestion and increased to 6.99 ± 0.08% after 2 h digestion (Fig. 4). There was then a large increase in curcumin release under *in vitro* small intestine conditions. The release percentage of curcumin from the particles reached around 69.5 ± 1.5% after 20 min digestion and 80.3 ± 3.3% by the end of the digestion period. The high bioaccessibility of the encapsulated curcumin than the non-encapsulated curcumin (even though the two systems had the same overall composition) can be attributed to differences in the initial location of the curcumin molecules in the systems. In the non-encapsulated system, the curcumin is initially present in a crystalline form that is difficult to dissolve. In the encapsulated system, the curcumin is an amorphous form as testified by XRD (Fig. 2A) and is initially dispersed throughout the zein matrix inside the nanoparticles. In the stomach and small intestine, proteases digest zein and sodium caseinate and convert proteins to peptides. The curcumin is then released at the same time as the peptides are formed, which may facilitate their interaction with each other and the formation of soluble complexes, which results in a higher bioaccessibility (Yao et al., 2018). In another study, it was reported that curcumin was mainly released under simulated gastric conditions (56%) from zein/NaCas-alginate nanoparticles prepared using an antisolvent method using ethanol (Liu et al., 2019). The result may indicate that the nature of the nanoparticles formed by ethanol or pH-shift methods may be different. Alternatively, the observed differences in curcumin release may have been due to differences in the simulated gastrointestinal models used in the studies.

In our study, the curcumin concentrations measured in the final digestion supernatant were 439 ± 17 and 76.7 ± 5.6 μM for the encapsulated and non-encapsulated formulations, respectively. Thus, encapsulation increased the bioaccessibility of the curcumin by about 5.7-fold.

3.5. *In vitro* antioxidant capacity of digested samples

The *in vitro* antioxidant capacities of the *in vitro* digestion supernatants of the encapsulated and non-encapsulated curcumin formulations were evaluated by measuring their abilities to scavenge DPPH· (Fig. 5A) and $ABTS^{+}$· radicals (Fig. 5B). The DPPH· scavenging abilities of the digested non-encapsulated and encapsulated curcumin formulations were 0.58 ± 0.01 and 2.18 ± 0.14 mM AAE, respectively (Fig. 5A), while the $ABTS^{+}$· scavenging abilities were 9.80 ± 0.79 and 3.05 ± 0.81 mM TEC, respectively (Fig. 5B). These results clearly show that curcumin has a considerably higher potency after encapsulation. The greater

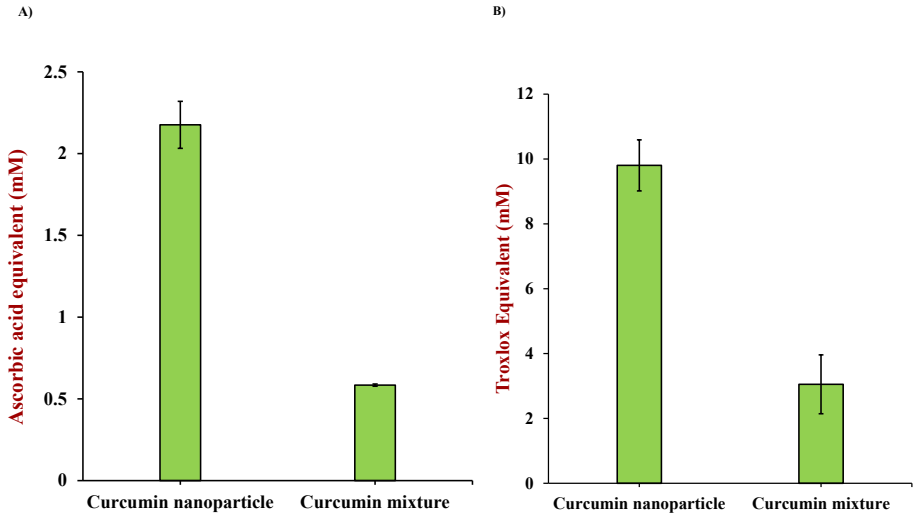

Fig. 5. *In vitro* antioxidant activity of gastrointestinal fluids collected after digestion of encapsulated and non-encapsulated curcumin formulations; A), DPPH· scavenging capacity expressed as ascorbic acid equivalents (mM); B), $ABTS^{+}$· scavenging capacity expressed as Trolox equivalents (mM).

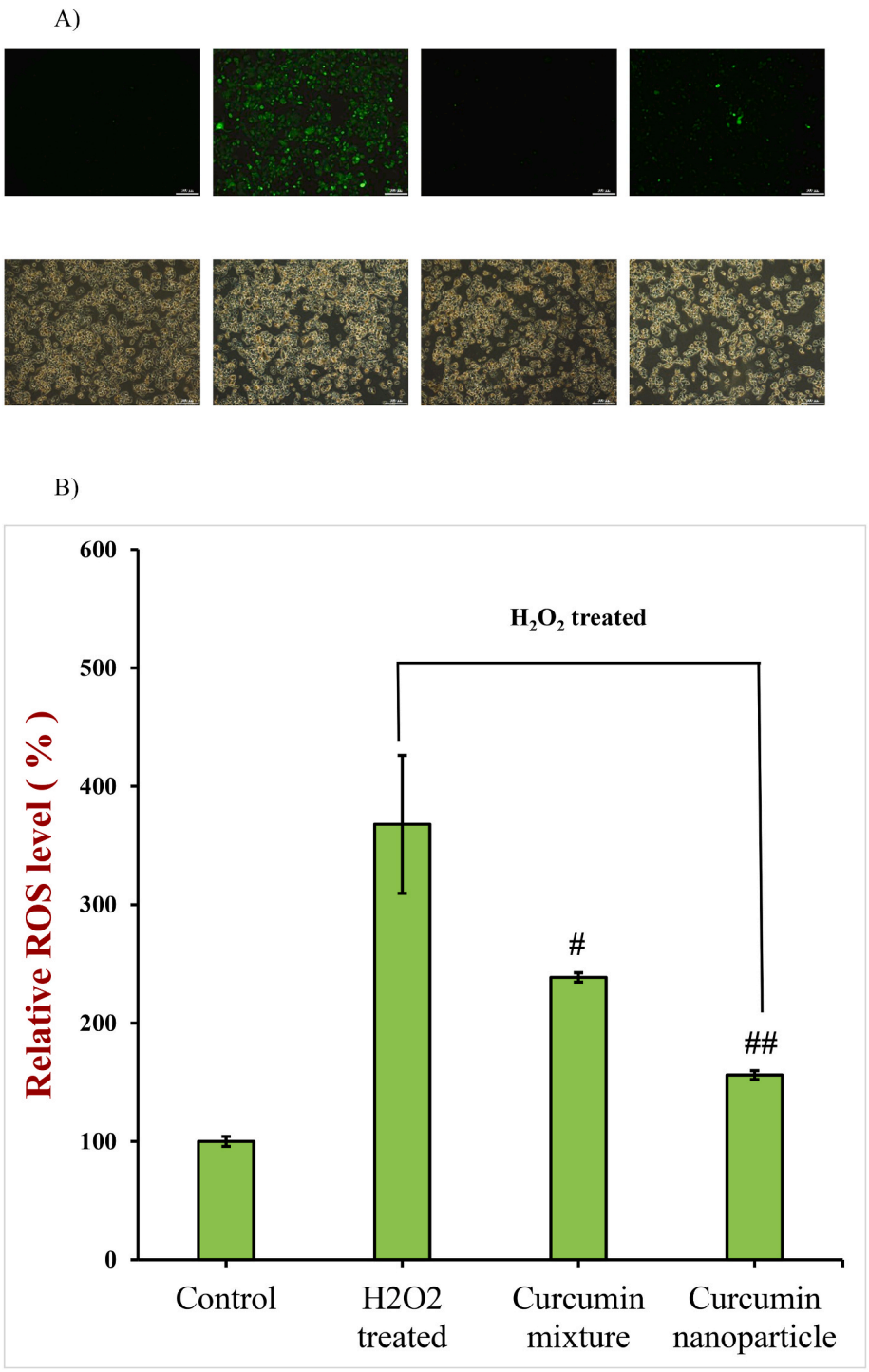

Fig. 6. Images (A) and fluorescence intensity (B) of control group (Control), H_2O_2-treated group, and H_2O_2-treated group after incubation with gastrointestinal fluids collected after digestion of encapsulated and non-encapsulated curcumin formulations. The higher the fluorescence intensity, the higher the ROS level (#, $P < 0.05$; ##, $P < 0.001$; compared to H_2O_2 group).

in vitro antioxidant activity of the encapsulated curcumin can be attributed to the higher concentration of soluble curcumin in the *in vitro* gastrointestinal digestion supernatant, as shown by the higher bioaccessibility reported in the previous section.

3.6. ROS scavenging capacity of digested nanoparticles

In vitro antioxidant activity assays may not accurately reflect the antioxidant activity of curcumin after absorption into cells. For this reason, we investigated the ROS scavenging capacity of the *in vitro* digested nanoparticles using HepG2 cells. Initially, the impact of the two curcumin formulations on the cytotoxicity of these cells was assessed (Fig. S1). The cell viability was only 1.2% and 35.1% when treated with digestion fluids collected from encapsulated (loaded in nanoparticles) and non-encapsulated (curcumin mixture) that were only diluted 10-fold, indicating that high levels of soluble curcumin may damage these cells. However, the cell viability increased substantially when the digestion supernatant was diluted more, exceeding 99% when they were

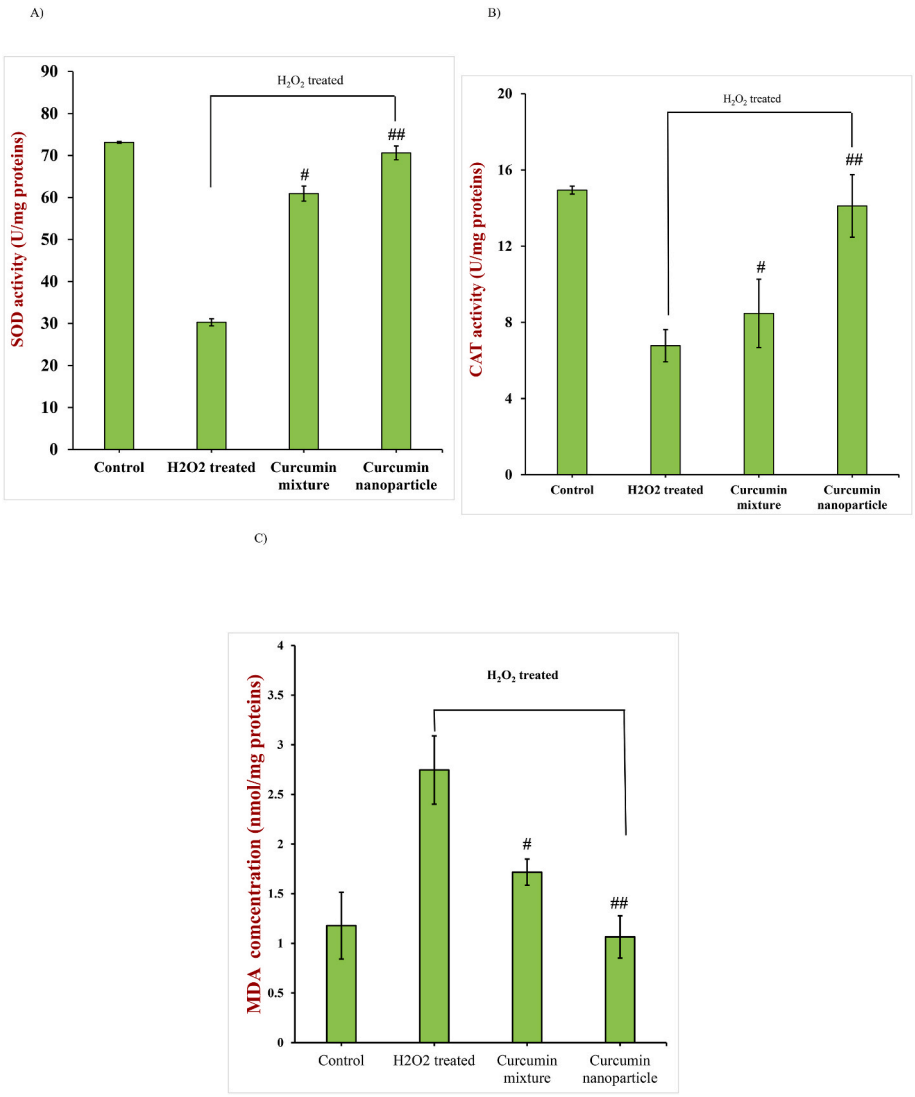

Fig. 7. SOD (A), CAT (B), and MDA (C) levels of control group (Control), H_2O_2 treated group, and H_2O_2-treated group after incubation with gastrointestinal fluids collected after digestion of encapsulated and non-encapsulated curcumin formulations. (#, $p < 0.05$; ##, $P < 0.001$; compared to H_2O_2 group).

diluted 50-fold. For this reason, all samples were diluted 50-fold prior to analyzing their ROS scavenging capacity. At this dilution level, the digested samples contained 8.78 and 1.53 μM curcumin for the encapsulated and non-encapsulated formulations, respectively.

Reactive oxygen scavenging species include hydrogen peroxide, superoxide radical, singlet oxygen, and hydroxyl free radical, which produce in normal cells (Kenneth Hensley et al., 2000). Moderate levels of ROS are required to regulate cell survival, but excessive ROS levels can oxidize cellular membrane lipids, nucleic acids, and proteins, which can have adverse health effects (Valko et al., 2007; Huang et al., 2019). In this study, hydrogen peroxide (H_2O_2) was used to promote oxidative stress in the HepG2 cells. A strong fluorescence signal was present in H_2O_2 treated HepG2 cells (Fig. 6A), while the control cells had a very weak signal, which meant that there was low level of ROS in normal cells, and H_2O_2 treatment produced excessive ROS in cells. The fluorescence signal decreased remarkably when treated with digested curcumin formulations then treated with H_2O_2 treatment (Fig. 5A), specially, after being treated with the *in vitro* digested encapsulated curcumin formulation ($P < 0.05$, Fig. 6B). These results indicated that the digestion supernatant of nanoparticles was more talent in scavenging intracellular ROS, which was reasonable since there was a higher level of soluble curcumin in the gastrointestinal fluids of encapsulated nanoparticles.

3.7. Cellular antioxidant capacity of digestion supernatant

The oxidative stress induced by H_2O_2 is normally reduced by the intracellular enzymatic antioxidants, which includes SOD and CAT enzymes. SOD catalyzes the reduction of superoxide anions into hydrogen peroxide, and then hydrogen peroxide and the other peroxides are reduced by CAT (Poprac et al., 2017; Liang et al., 2022). A reduction in their activity is an indication of an increase in intracellular oxidative stress.

As expected, the activity of SOD was higher in the control cells (73.1 ± 1.5 U/mg protein) than the H_2O_2-treated cells (30.3 ± 2.0 U/mg protein) (Fig. 7A), which indicated that oxidative stress inhibited SOD activity in the cells. The enzyme activity in the H_2O_2-treated cells increased significantly when they were exposed to the digested curcumin formulations ($P < 0.05$), being 70.6 ± 4.5 and 60.9 ± 1.8 U/mg proteins for the encapsulated and non-encapsulated systems, respectively. Indeed, the SOD activity for the encapsulated systems almost approached that for the control cells.

The CAT activity (Fig. 7B) was significantly higher (14.9 ± 0.2 U/mg protein) in the control cells than in the H_2O_2-treated ones (6.8 ± 0.8 U/mg proteins), which again shows that hydrogen peroxide decreased the normal activity of the antioxidant enzymes. Incubation of the H_2O_2-cells with the *in vitro* digested curcumin formulations significantly ($P < 0.05$)

increased the CAT activity, with the extent of this increase being much greater for the encapsulated system (14.1 ± 1.6 U/mg protein) than the non-encapsulated one (8.5 ± 1.8 U/mg protein). Indeed, the encapsulated curcumin brought the CAT activity back to the level found in the control, thereby reducing the damaging effects of oxidative stress caused by the H_2O_2. The higher efficacy of the digested fluids collected from the encapsulated curcumin formulation can be attributed to the higher concentration of soluble curcumin present.

MDA is a secondary reaction product of lipid oxidation, which is often used as a biomarker of lipid peroxidation inside cells (Rong et al., 2012). The MDA concentration of the H_2O_2-treated HepG2 cells was around 2.5-fold higher than that of the control cells (Fig. 7C). Both curcumin formulations reduced the level of MDA produced, but again the encapsulated curcumin was significantly more effective than the non-encapsulated one ($P < 0.05$), which can be attributed to the reasons discussed earlier.

4. Conclusions

In summary, we successfully fabricated curcumin-loaded zein/caseinate-alginate nanoparticles with high curcumin loading efficiency (83.1%) using a pH-shift/electrostatic deposition method. The main advantages of this method are its simplicity, affordability, and avoidance of ethanol use. The nanoparticles were stable against aggregating over a pH range of 2.0–7.3 and high salt concentration of 1.6 M, which means they could be used in acid to neutral food products. Under *in vitro* simulated gastric conditions, the nanoparticles tended to aggregate, which was attributed to protonation of the alginate coating under strongly acidic conditions, which protected the nanoparticles from digestion, thereby retaining most of the curcumin inside them. Under *in vitro* simulated small intestine conditions, the curcumin was rapidly released, reaching a bioaccessibility of around 80.3% by the end of digestion. The bioaccessibility of the curcumin was much higher when it was encapsulated in nanoparticles, rather than free curcumin, which can be attributed to an amorphous form of curcumin in the nanoparticles. Encapsulation curcumin with nanoparticles was shown to greatly increase its *in vitro* and intracellular antioxidant activity, which was mainly attributed to the higher concentration of soluble curcumin in the gastrointestinal fluids after digestion. Overall, our results suggest that zein/caseinate-alginate nanoparticles may be an effective encapsulation technology for delivering curcumin (and other antioxidant polyphenols) to the small intestine. Consequently, they could be utilized in functional food, nutraceutical supplement, and drugs.

CRediT authorship contribution statement

Yunfei Huang: Project administration, Investigation, Methodology, Writing – original draft. **Yiling Zhan:** particle stability experiments. **Guangyi Luo:** Data curation, digestion. **Yan Zeng:** Software, Formal analysis. **David Julian McClements:** Conceptualization, Supervision, Writing – review & editing. **Kun Hu:** Conceptualization, Resources, Funding acquisition.

Declaration of competing interest

The authors declare the following financial interests/personal relationships which may be considered as potential competing interests: Kun Hu reports financial support was provided by National Natural Science Foundation of China.

Data availability

Data will be made available on request.

Acknowledgements

This work was funded by the National Natural Science Foundation of China (No. 31771920).

Appendix A. Supplementary data

Supplementary data to this article can be found online at https://doi.org/10.1016/j.crfs.2023.100463.

References

Ak, T., Gulcin, I., 2008. Antioxidant and radical scavenging properties of curcumin. Chem. Biol. Interact. 174 (1), 27–37. Available from: https://www.ncbi.nlm.nih.gov/pubmed/18547552.

Anand, P., Kunnumakkara, A.B., Newman, R.A., Aggarwal, B.B., 2007. Bioavailability of curcumin: problems and promises. Mol. Pharm. 4 (6), 807–818. Available from: https://pubs.acs.org/doi/pdf/10.1021/mp700113r.

Chang, C., Wang, T., Hu, Q., Luo, Y., 2017. Caseinate-zein-polysaccharide complex nanoparticles as potential oral delivery vehicles for curcumin: effect of polysaccharide type and chemical cross-linking. Food Hydrocolloids 72, 254–262. https://doi.org/10.1016/j.foodhyd.2017.05.039.

Dai, L., Li, R., Wei, Y., Sun, C., Mao, L., Gao, Y., 2018. Fabrication of zein and rhamnolipid complex nanoparticles to enhance the stability and invitro release of curcumin. Food Hydrocolloids 617–628. Available from: https://www.sciencedirect.com/science/article/pii/S0268005X17312419?via%3Dihub.

Dai, L., Sun, C., Li, R., Mao, L., Liu, F., Gao, Y., 2017. Structural characterization, formation mechanism and stability of curcumin in zein-lecithin composite nanoparticles fabricated by antisolvent co-precipitation. Food Chem. 237, 1163–1171. Available from: https://www.ncbi.nlm.nih.gov/pubmed/28763965.

Ghobadi-Oghaz, N., Asoodeh, A., Mohammadi, M., 2022. Fabrication, characterization and in vitro cell exposure study of zein-chitosan nanoparticles for co-delivery of curcumin and berberine. Int. J. Biol. Macromol. 204, 576–586. Available from: https://www.ncbi.nlm.nih.gov/pubmed/35157902.

Hasankhan, S., Tabibiazar, M., Hosseini, S.M., Ehsani, A., Ghorbani, M., 2020. Fabrication of curcumin-zein-ethyl cellulose composite nanoparticles using antisolvent co-precipitation method. Int. J. Biol. Macromol. 163, 1538–1545. Available from: https://www.ncbi.nlm.nih.gov/pubmed/32784024.

Hu, K., Huang, X., Gao, Y., Huang, X., Xiao, H., McClements, D.J., 2015. Core-shell biopolymer nanoparticle delivery systems: synthesis and characterization of curcumin fortified zein-pectin nanoparticles. Food Chem. 182, 275–281. Available from: https://www.ncbi.nlm.nih.gov/pubmed/25842338.

Hu, K., McClements, D.J., 2015. Fabrication of biopolymer nanoparticles by antisolvent precipitation and electrostatic deposition: zein-alginate core/shell nanoparticles. Food Hydrocolloids 44, 101–108. https://doi.org/10.1016/j.foodhyd.2014.09.015.

Huang, X., Huang, X., Gong, Y., Xiao, H., McClements, D.J., Hu, K., 2016. Enhancement of curcumin water dispersibility and antioxidant activity using core-shell protein-polysaccharide nanoparticles. Food Res. Int. 87, 1–9. Available from: https://www.ncbi.nlm.nih.gov/pubmed/29606228 https://www.sciencedirect.com/science/article/pii/S0963996916302447?via%3Dihub.

Huang, X., Liu, Y., Zou, Y., Liang, X., Peng, Y., McClements, D.J., Hu, K., 2019. Encapsulation of resveratrol in zein/pectin core-shell nanoparticles: stability, bioaccessibility, and antioxidant capacity after simulated gastrointestinal digestion. Food Hydrocolloids 93, 261–269. https://doi.org/10.1016/j.foodhyd.2019.02.039.

Kenneth Hensley, K.A.R., Prasad Gabbita, S., Scott, Salsman, Floyd, Robert A., 2000. Reactive oxygen species, cell signaling, and cell injury. Free Radical Biol. Med. 28 (10), 1456–1462.

Li, M., Liu, Y., Liu, Y., Zhang, X., Han, D., Gong, J., 2022. Ph-driven self-assembly of alcohol-free curcumin-loaded zein-propylene glycol alginate complex nanoparticles. Int. J. Biol. Macromol. 213, 1057–1067. Available from: https://www.ncbi.nlm.nih.gov/pubmed/35691429.

Liang, X., Cao, K., Li, W., Li, X., McClements, D.J., Hu, K., 2021. Tannic acid-fortified zein-pectin nanoparticles: stability, properties, antioxidant activity, and in vitro digestion. Food Res. Int. 145, 110425. Available from: https://www.ncbi.nlm.nih.gov/pubmed/34112427.

Liang, X., Cheng, W., Liang, Z., Zhan, Y., McClements, D.J., Hu, K., 2022. Co-encapsulation of tannic acid and resveratrol in zein/pectin nanoparticles: stability, antioxidant activity, and bioaccessibility. Foods 11 (21). Available from: https://www.ncbi.nlm.nih.gov/pubmed/36360091.

Liu, Q., Jing, Y., Han, C., Zhang, H., Tian, Y., 2019. Encapsulation of curcumin in zein/caseinate/sodium alginate nanoparticles with improved physicochemical and controlled release properties. Food Hydrocolloids 93, 432–442. https://doi.org/10.1016/j.foodhyd.2019.02.003.

Liu, Z., Smart, J.D., Pannala, A.S., 2020. Recent developments in formulation design for improving oral bioavailability of curcumin: a review. J. Drug Deliv. Sci. Technol. 60. Available from: https://www.sciencedirect.com/science/article/pii/S177322472031371X?via%3Dihub.

Pan, K., Luo, Y., Gan, Y., Baek, S.J., Zhong, Q., 2014. Ph-driven encapsulation of curcumin in self-assembled casein nanoparticles for enhanced dispersibility and bioactivity. Soft Matter 10 (35), 6820–6830. Available from: https://www.ncbi.nlm.nih.gov/pubmed/25082426.

Pan, K., Zhong, Q., 2016. Low energy, organic solvent-free co-assembly of zein and caseinate to prepare stable dispersions. Food Hydrocolloids 52, 600–606. https://doi.org/10.1016/j.foodhyd.2015.08.014.

Patel, A.R., Bouwens, E.C., Velikov, K.P., 2010. Sodium caseinate stabilized zein colloidal particles. J. Agric. Food Chem. 58 (23), 12497–12503. Available from: https://www.ncbi.nlm.nih.gov/pubmed/21077613.

Peng, S., Zhou, L., Cai, Q., Zou, L., Liu, C., Liu, W., McClements, D.J., 2020. Utilization of biopolymers to stabilize curcumin nanoparticles prepared by the ph-shift method: caseinate, whey protein, soy protein and gum Arabic. Food Hydrocolloids 107. https://doi.org/10.1016/j.foodhyd.2020.105963.

Peng, Y., Li, X., Gu, P., Cheng, W., Zhang, R., Hu, K., 2022. Curcumin-loaded zein/pectin nanoparticles: caco-2 cellular uptake and the effects on cell cycle arrest and apoptosis of human hepatoma cells (hepg2). J. Drug Deliv. Sci. Technol. 74 https://doi.org/10.1016/j.jddst.2022.103497.

Poprac, P., Jomova, K., Simunkova, M., Kollar, V., Rhodes, C.J., Valko, M., 2017. Targeting free radicals in oxidative stress-related human diseases. Trends Pharmacol. Sci. 38 (7), 592–607. Available from: https://www.ncbi.nlm.nih.gov/pubmed/28551354.

Rauf, A., Imran, M., Orhan, I.E., Bawazeer, S., 2018. Health perspectives of a bioactive compound curcumin: a review. Trends Food Sci. Technol. 74, 33–45. https://doi.org/10.1016/j.tifs.2018.01.016.

Rong, S., Zhao, Y., Bao, W., Xiao, X., Wang, D., Nussler, A.K., Yan, H., Yao, P., Liu, L., 2012. Curcumin prevents chronic alcohol-induced liver disease involving decreasing ros generation and enhancing antioxidative capacity. Phytomedicine 19 (6), 545–550. Available from: https://www.ncbi.nlm.nih.gov/pubmed/22445643.

Sahebkar, A., 2016. Curcumin: a natural multitarget treatment for pancreatic cancer. Integr. Cancer Ther. 15 (3), 333–334. Available from: https://www.ncbi.nlm.nih.gov/pubmed/26867801 https://www.ncbi.nlm.nih.gov/pmc/articles/PMC5739188/pdf/10.1177_1534735415624139.pdf.

Sani, M.A., Tavassoli, M., Azizi-Lalabadi, M., Mohammadi, K., McClements, D.J., 2022. Nano-enabled plant-based colloidal delivery systems for bioactive agents in foods: design, formulation, and application. Adv. Colloid Interface Sci. 305, 102709. Available from: https://www.ncbi.nlm.nih.gov/pubmed/35640316.

Shukla, R., 2001. Zein the industrial protein from corn. Ind. Crop. Prod. 13, 171–192.

Sun, J., Bi, C., Chan, H.M., Sun, S., Zhang, Q., Zheng, Y., 2013. Curcumin-loaded solid lipid nanoparticles have prolonged in vitro antitumour activity, cellular uptake and improved in vivo bioavailability. Colloids Surf. B Biointerfaces 111, 367–375. Available from: https://www.ncbi.nlm.nih.gov/pubmed/23856543.

Valko, M., Leibfritz, D., Moncol, J., Cronin, M.T., Mazur, M., Telser, J., 2007. Free radicals and antioxidants in normal physiological functions and human disease. Int. J. Biochem. Cell Biol. 39 (1), 44–84. Available from: http://www.ncbi.nlm.nih.gov/pubmed/16978905.

Wang, X., Huang, H., Chu, X., Han, Y., Li, M., Li, G., Liu, X., 2019. Encapsulation and binding properties of curcumin in zein particles stabilized by tween 20. Colloids Surf. A Physicochem. Eng. Asp. 577, 274–280. https://doi.org/10.1016/j.colsurfa.2019.05.094.

Yao, K., Chen, W., Song, F., McClements, D.J., Hu, K., 2018. Tailoring zein nanoparticle functionality using biopolymer coatings: impact on curcumin bioaccessibility and antioxidant capacity under simulated gastrointestinal conditions. Food Hydrocolloids 79, 262–272. https://doi.org/10.1016/j.foodhyd.2017.12.029.

Yuan, Y., Xiao, J., Zhang, P., Ma, M., Wang, D., Xu, Y., 2021. Development of ph-driven zein/tea saponin composite nanoparticles for encapsulation and oral delivery of curcumin. Food Chem. 364, 130401. Available from: https://www.ncbi.nlm.nih.gov/pubmed/34174648.

Zhan, X., Dai, L., Zhang, L., Gao, Y., 2020. Entrapment of curcumin in whey protein isolate and zein composite nanoparticles using ph-driven method. Food Hydrocolloids 106. https://doi.org/10.1016/j.foodhyd.2020.105839.

Zhang, D., Jiang, F., Ling, J., Ouyang, X.K., Wang, Y.G., 2021. Delivery of Curcumin Using a Zein-Xanthan Gum Nanocomplex: Fabrication, Characterization, and in Vitro Release Properties, vol. 204. Colloids Surf B Biointerfaces, 111827. Available from: https://www.ncbi.nlm.nih.gov/pubmed/33984612.

Zhu, J.J., Tang, C.H., Luo, F.C., Yin, S.W., Yang, X.Q., 2022. Topical application of zein-silk sericin nanoparticles loaded with curcumin for improved therapy of dermatitis. Mater. Today Chem. 24 https://doi.org/10.1016/j.mtchem.2022.100802.

Zou, Y., Qian, Y., Rong, X., Cao, K., McClements, D.J., Hu, K., 2021. Encapsulation of quercetin in biopolymer-coated zein nanoparticles: formation, stability, antioxidant capacity, and bioaccessibility. Food Hydrocolloids 120. https://doi.org/10.1016/j.foodhyd.2021.106980.